

Humidity Sensing Properties of $\text{Bi}_{0.5}\text{Na}_{0.25}\text{Li}_{0.25}\text{TiO}_3$ Ceramics

A Thesis Submitted

In partial fulfillment of the requirement

For the degree of

BACHELOR OF TECHNOLOGY

Submitted by:

KUMAR SHUBHAM

ROLL NO-110CR0630

SUPERVISOR:

PROF. J.BERA



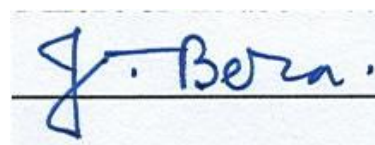
**DEPARTMENT OF CERAMIC ENGINEERING,
NATIONAL INSTITUTE OF TECHNOLOGY ROURKELA, ROURKELA-769008**

MAY 2014

CERTIFICATE

This is certified that the work contained in the project entitled “Humidity Sensing Properties of $\text{Bi}_{0.5}\text{Na}_{0.25}\text{Li}_{0.25}\text{TiO}_3$ Ceramics” by Kumar Shubham (Roll 110CR0630), in partial fulfilment of the requirements of the award of Bachelor of Technology Degree in Ceramic Engineering at the National Institute of Technology, Rourkela is an authentic work carried out by him under my supervision and guidance.

To the best of my knowledge, the matter embodied in the thesis has not been submitted to any other university / institute for the award of any Degree or Diploma.

A handwritten signature in blue ink, reading "J. Bera.", is written over a horizontal line.

Date: 12.05.2014

(JAPES BERA)

ASSOCIATE PROFESSOR

Department of Ceramic Engineering

ACKNOWLEDGEMENT

The success and final outcome of this project required a lot of guidance and assistance from many people and I am extremely fortunate to have got this all along the completion of my project work. Whatever I have done is only due to such guidance and assistance and I would not forget to thank them.

I owe my profound gratitude to my project guide **Prof. Japes Bera, department of ceramic engineering, Rourkela** who took keen interest in my project work and guided me all along, till the completion of my project work by providing all the necessary information and dynamic suggestions. His hawk-eyed supervision amalgamated with eternal inspiration and support are the pillars behind this project.

I would not forget to remember **Ms. Geeta** for their unlisted encouragement and more over for their timely support and guidance till the completion of our project work.

Kumar Shubham

110CR0630

List of figures

SLNO.	FIGURE CAPTION
Figure 1.1	Types of humidity sensors
Figure 1.2:	Pervskite crystal structure.
Figure 2.1	Bragg's law
Figure 2.2	Pallets electroding
Figure: 2.3	Pallets in the desiccator
Figure 2.4	Controlled Humid environment
Figure 2.5	Impedance analysis device
Figure 3.1	XRD of $\text{Bi}_{0.5}\text{Na}_{0.5}\text{TiO}_3$
Figure 3.2	XRD of $\text{Bi}_{0.5}\text{Li}_{0.5}\text{TiO}_3$
Figure 3.3	XRD of $\text{Bi}_{0.5}\text{Na}_{0.25}\text{Li}_{0.25}\text{TiO}_3$
Figure 3.4	800°C SEM micrograph
Figure 3.5	850°C SEM micrograph
Figure 3.6	900°C SEM micrograph
Figure 3.7	Impedance spectra at 33% RH
Figure 3.8	Impedance spectra at 75% RH
Figure 3.9:	Impedance spectra at 85% RH
Figure 3.10	Equivalent circuit design
Figure 3.11	Impedance versus RH

TABLE CAPTION

SLNO.

Table 2.1	supersaturated aqueous solution and equivalent relative humidity
-----------	--

Table 2.2	Supersaturated salt versus amount required per 100 ml
-----------	---

Table 3.1	Apparent porosity and bulk density
-----------	------------------------------------

CONTENTS

1 :	INTRODUCTION AND BACKGROUND 1.1 TYPES OF HUMIDITY 1.2 TYPES OF HUMIDITY SENSORS 1.3 SENSING MECHANISM 1.4 ABO ₃ STRUCTURE AND SENSING PROPERTIES	
2 :	EXPERIMENTAL WORK 2.1 MATERIAL SYNTHESIS AND PROCESSING 2.1.1 RAW MATERIALS 2.1.2 BATCH CALCULATION 2.1.3 BATCH PREPARATION 2.1.4 DRYING AND GRINDING 2.1.5 SHAPING AND FIRING 2.2 CHARACTERISATION 2.2.1 DETERMINATION OF A.P AND B.D 2.2.2 XRD ANALYSIS 2.2.3 SEM ANALYSIS 2.3 SILVER COATING OF THE SAMPLE 2.4 COPPER WIRE ELECTRODING 2.5 CREATION OF CONTROLLED HUMIDITY ENVIRONMENT	

	2.6 HUMIDITY SENSING TETST	
	2.7 FLOW DIAGRAM FOR COMPLETE PROCESS	
3 :	RESULT AND DISSCUSSION 3.1 APPARENT POROSITY AND BULK DENSITY 3.2 XRD ANALYSIS 3.3 SEM ANALYSIS 3.3.1 SEM OF SAMPLE SINTERED AT 800°C 3.3.2 SEM OF SAMPLES SINTERED AT 850°C 3.3.2 SEM OF SAMPLES SINTERED AT 900°C 3.4 HUMIDITY SENSING MECHANISM AND CHARACTERSTICS GRAPHS	
4 :	CONCLUSION	
References :		

1.1 Introduction and Background

In simple terms, we can define the presence of water in air as humidity, while a ‘hygrometer’ or humidity sensor is an instrument that measures the humidity or moisture content in the atmosphere. The water vapor content in the air can have negative impact on human comfort as well as industrial manufacturing processes [1]. The water vapor presence can also influence myriad chemical, physical and biological processes. In industries, measuring humidity is very essential because not only it can increase the business price of the selling product but, also inhibit safety and health of workers. Thus, humidity sensing plays an important role in control system for industrial processes and comfort of humans [2].

Principle utility of a humidity sensor is measuring relative humidity variations around. Measuring relative humidity will include the estimation of temperature around as well as moistness. The ratio of true moisture existing in the air to the maximum level of dampness present in the air at the same temperature is known as ‘relative humidity’. The fractional value thus obtained is converted to percentage and that is how relative humidity is expressed: percentage ratio of actual moisture to maximum moisture at a definite temperature in the air. The relative humidity varies with temperature variation because warmer air can hold more moisture than the colder one [1]. Any form of water vapor like precipitation, fog or dew increases the humidity content in the air [3].

Checking, monitoring and controlling humidity is very important in most domestic and industrial sectors. At the time of wafer processing, humidity needs to be controlled in semiconductor industry. In respiratory instruments, pharmaceutical

equipments, incubators, sterilizers, and other medical instruments, maintaining an apt humidity is of paramount importance [3, 4]. Humidity control is necessitated in chemical industries when gas purification is taking place, or during film desiccation, food processing and textile production. In agricultural sector also monitoring humidity becomes vital for plant protection and dew inhibition. A phenomena called heat index takes place when more water molecules in the air diminishes the efficiency of sweating for cooling the body by shrinking down the rate of evaporation of moisture from epidermal layer of skin [5].

Broadly, humidity measurement is expressed in three different ways:

- a) Absolute Humidity
- b) Relative Humidity
- c) Specific Humidity

1.2. Types of humidity

Absolute humidity :

Absolute humidity can be defined as the total mass of water vapor in a unit volume of mixture of total air and vapor. It is expressed as:

$$\text{Absolute Humidity} = M_{\text{Water}}/P_{\text{total}}$$

It ranges from being zero to as high as approximately thirty grams in a cubic meter when the air is saturated at the temperature of thirty degrees [2].

As the temperature or weight of air alters, the moisture content in it changes too. This is not required for synthetic designing like for drying dresses where there are chances of temperature fluctuations. Volume stickiness is the measure of mass of water for each single unit volume. Thus total humidity can be calculated as the average cumulative sum of all the water vapor introduced in a particular volume of air [2].

Relative humidity:

The fractional ratio of the amount of moisture contained in the air to the maximum possible amount of moisture containable in the air at a particular temperature is defined as relative humidity. This is however converted to percentage by multiplying the fractional value by hundred. The level of the midway weight of moisture in the mix to immersed moisture weight defines the relative moistness in a mixture of air and water. Thus both the water as well as temperature characterizes the relative moistness of air [2].

Mathematically, relative moistness is expressed as rate by the following formula:

$$\phi = \frac{e_w}{e^*_w} \times 100\%$$

Relative humidity is very important for estimation related to climates, as it considers the precipitation, dew and mist in its calculations. The popular belief of air holding the water vapor for describing relative humidity is a misconception. Even in air-less volume, water vapor can be contained and humidity can be calculated for this air-less volume [2].

Specific humidity:

Specific humidity is the ratio of water vapor and single mass of dry air in a mixture of particular volume. It is roughly equivalent to the “ratio of mixing” which is mass of water vapor in the air divided by mass of dry air of same volume [2].

Specific Humidity is mathematically expressed as:

$$SH = \frac{m_v}{(m_v + m_a)}.$$

Specific humidity can also be calculated as:

$$SH = \frac{0.622p_{(H_2O)}}{P_{(dry\ air)}}$$
$$0.622 = \frac{MM_{H_2O}}{MM_{dry\ air}}$$

or:

$$SH = \frac{0.622p_{(H_2O)}}{p - 0.378 * p_{(H_2O)}}.$$

By this definition of specific humidity, the relative humidity can be represented as :

$$\phi = \frac{SH * p}{(0.622 + 0.378 * SH)p_{(H_2O)}^*} \times 100$$

1.3. Types of humidity sensors

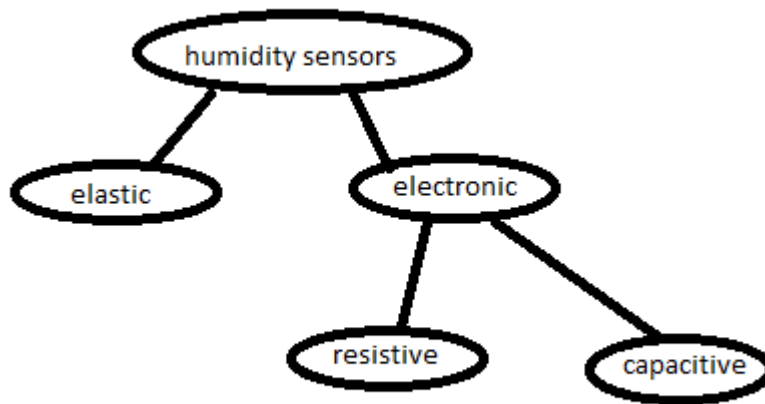


Figure 1.1. Types of humidity sensor

Humidity sensors are broadly classified into two categories:

- a) elastic humidity sensors
- b) electronic humidity sensors

Resistive humidity sensors:

In these types, the resistance of the material varies with humidity and thus by proper calibration of the results, humidity is measured. Alumina and thermoplastics are the most common materials used for these kinds of material. Accuracy, slow response time and bad sensing time are some of the demerits [1,2].

Capacitive humidity sensors:

For parallel plate capacitor, capacitance is given by:

$$C = \epsilon_0 \epsilon_r A / D$$

where, C = capacitance

ϵ_0 = free space permittivity

ϵ_r = dielectric permittivity

A = plates area

D = inter-plate distance

In capacitive type humidity sensors, when moisture is absorbed, the parameters on the right sides of the equation will change and thus the capacitance will vary. So for different humidity, we will be having different capacitance values. Materials like polymers and polyesters are used for fabricating these types of capacitors. These sensors have shown better response time, linearity and high response accuracy [2-4].

1.4. Sensing mechanism

A dielectric material is placed in between a pair of electrodes forming a capacitor. With dielectric constant in between 2 and 15, plastic, polymer or ceramics are generally used as dielectric material. Water vapor dielectric value is 80 at the room temperature, which is very large than that shown by dielectric without moisture, thus making sensor work.

After absorbing water, the porous material electrical properties are altered. Water molecules are retained on active oxide surfaces and form hydroxyl ions by

dissociation mechanism. While, if this happens on the surface of a metal, the local density and electric field is changed and the proton reacts with oxygen to form hydroxyl ions [5].

1.5. ABO_3 structure and sensing properties

ABO_3 is perovskite structure in which A are rare earth metals, alkali or alkaline earth metal, and B are transition metals.

Perovskite structure have shown excellent stability in thermal and catalytic activities. The cost of making humidity sensors is reduced and processing is cheaper.

Also in the structure of perovskite, fig 1.2, the susceptibility of atom on the A site is large for humidity sensing so they have been replaced by alkaline earth metals [6].

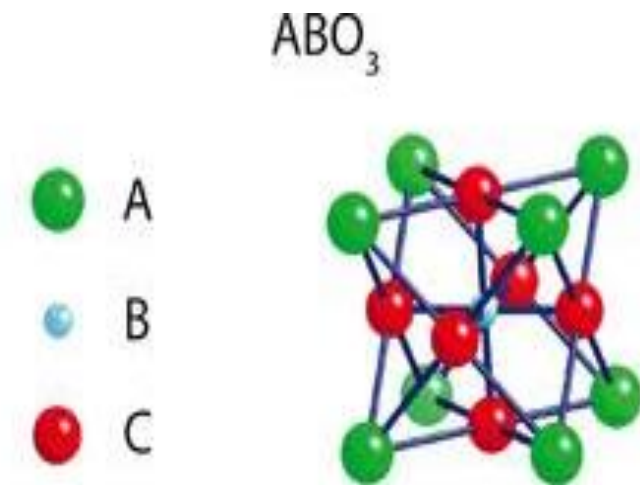


Figure 1.2. Perovskite unit cell structure [6]

Because ceramic sensors are cheaper and easier in fabrication, they found use for the fabrication materials for making humidity sensor. The simple structure of ceramic sensors makes them easy to process. The change of dielectric constant is the reason for sensing mechanism in ceramic sensors. This alteration of dielectric constant is associated with simultaneous change in capacitance which alludes to the humidity change. The time taken for sensing is dependent on the geometry of the sensor, hence high surface area and high porosity are very necessary as higher the surface area and higher the porosity, higher will be the active sites for humidity absorption [2-4, 7].

Earlier ABO_3 -type complex metal oxides with the substitution of A-site ions like $\text{Bi}_{0.5}\text{K}_{0.5}\text{TiO}_3$ have been studied and found out to be novel material for humidity sensing. They have tetragonal structure at room temperature. Because of low coercive field ($E_c = 1.5 \times 10^3 \text{ V/mm}$), and high Curie temperature ($T_c = 380^\circ\text{C}$) lead-free chemical composition and excellent electrical properties [8] and, they have been studied.

Both $\text{Bi}_{0.5}\text{Na}_{0.5}\text{TiO}_3$ and $\text{Bi}_{0.5}\text{Li}_{0.5}\text{TiO}_3$ are ABO_3 -type complex metal oxides with the substitution of A-site ions. This work aims at understanding the effect of substitution of A-site ions by two alkaline earth metals and preparation of $\text{Bi}_{0.5}\text{Na}_{0.25}\text{Li}_{0.25}\text{TiO}_3$ based ceramic humidity sensor. The effects of substitution of A-site by two alkaline earth metals on humidity sensing properties were investigated and sensing mechanism was explored. These researches may help in offering important and useful guidelines to design humidity sensors and understand the co-substitution effects at the A-site [9].

2. EXPERIMENTAL

2.1. Material synthesis and processing

2.1.1. Raw materials used:

For preparation of $\text{Bi}_{0.5}\text{Na}_{0.5}\text{TiO}_3$, the raw materials used were TiO_2 , Bi_2O_3 and Na_2CO_3 . Similarly for $\text{Bi}_{0.5}\text{Li}_{0.5}\text{TiO}_3$ the oxide used was Li_2O apart from TiO_2 and Bi_2O_3 . And for $\text{Bi}_{0.5}\text{Na}_{0.25}\text{Li}_{0.25}\text{TiO}_3$, all the aforementioned oxides were used.

2.1.2 Batch calculation:

To determine the correct mix of oxides in the mixture, batch calculation was done. Three compositions, each of 10 g were batched in the process.

For 10 g preparation of $\text{Bi}_{0.5}\text{Na}_{0.5}\text{TiO}_3$

1 mole $\text{TiO}_2 = 79.90 \text{ g} = 3.771 \text{ g in 10 g mix}$

0.25 mole $\text{Bi}_2\text{O}_3 = 116.49 \text{ g} = 5.498 \text{ g in 10 g mix}$

0.25 mole $\text{Na}_2\text{CO}_3 = 0.25 \text{ mole Na}_2\text{O} = 15.475 \text{ g} = 1.249 \text{ g in 10 g mix}$

$\text{Na}_2\text{CO}_3 \rightarrow \text{Na}_2\text{O} + \text{CO}_2$

For 10 g preparation of $\text{Bi}_{0.5}\text{Li}_{0.5}\text{TiO}_3$

1 mole $\text{TiO}_2 = 79.90 \text{ g} = 3.771 \text{ g in 10 g mix}$

0.25 mole $\text{Bi}_2\text{O}_3 = 116.49 \text{ g} = 5.59 \text{ g in 10 g mix}$

0.25 mole of $\text{Li}_2\text{O} = 14.93 \text{ g} = 0.706 \text{ g in 10 g mix}$

For 10 g preparation of $\text{Bi}_{0.5}\text{Na}_{0.25}\text{Li}_{0.25}\text{TiO}_3$

1 mole $\text{TiO}_2 = 79.90 \text{ g} = 3.91 \text{ g in } 10 \text{ g mix}$

0.25 mole $\text{Bi}_2\text{O}_3 = 116.49 \text{ g} = 5.6 \text{ g in } 10 \text{ g mix}$

0.125 mole of $\text{Li}_2\text{O} = 3.72 \text{ g} = 0.17 \text{ g in } 10 \text{ g mix}$

0.125 mole $\text{Na}_2\text{CO}_3 = 0.125 \text{ mole } \text{Na}_2\text{O} = 7.73 \text{ g} = 0.37 \text{ g in } 10 \text{ g mix}$

2.1.3. Batch preparation:

After the calculation of batch, the batch preparation was done via traditional solid sintering method. The apt amount of oxides and carbonates were weight and mixed in agate mortar for three hours till the mixture acquires a homogeneous color. The process was repeated for all the three mixture preparation.

2.1.4 Drying and grinding:

The samples were dried at 110^0 C in the drier and then they were grinded separately again in the agate mortar till the mixture is completely powdered.

2.1.5. Shaping and firing:

The powdered mixture were mixed with 5 volume % PVA solution and mixed thoroughly to get the uniform powder color again, till all the PVA solution is dried. Then the powdered samples were put in the die for pressing. With a load of 4.2 ton and soaking time of 60 seconds, the powdered samples were pressed into circular pallets of 12 mm diameter and 0.5 mm thickness.

Then the dried samples are fired at three different temperature which are 800°C for $\text{Bi}_{0.5}\text{Na}_{0.5}\text{TiO}_3$, 850°C for $\text{Bi}_{0.5}\text{Na}_{0.25}\text{Li}_{0.25}\text{TiO}_3$ and 900°C of $\text{Bi}_{0.5}\text{Li}_{0.5}\text{TiO}_3$ with soaking time of 6 hours.

2.2 CHARACTERISATION

We must determine the internal structure and properties of the material for its proper functioning and use. Thus, testing and inspection of ceramic material is very critical. The material must be porous as well as dense enough since porosity would determine the water absorption from the surface and hence give the humidity value after capacitive change. XRD has been done to get the phases present and for determination of atomic structure of the crystal.

2.2.1 Determination of Apparent porosity and Bulk density

Fired samples were weighted just after the firing and the weight is noted as dry weight (D). The dry pallets were then placed in a beaker and filled with water. After boiling the beaker on a heater for 4 hours, it is evacuated to a pressure less than 25mm of Hg. The pallets were retained in the reduced pressure for 5-6 hours. Then they were suspended with the help of pan I water and the suspended weight of the pallets was noted down as suspended weight(S). After wiping off the surface water completely with cotton, weight is measured again and this weight is noted down as soaked weight (W).

The apparent porosity (P) and bulk density (B) is mathematically expressed as:

$$P = \frac{W-D}{W-S} \times 100 (\%)$$

$$B = \frac{D}{W-S} \times$$

density of the media in which experiment is performed

In this case, water was the media.

2.2.2 XRD ANALYSIS

On passing X-rays through the matter, the interaction of electrons in the atoms of sample specimen and the radiation takes place which results in the scattering of X-rays. The crystalline materials have fixed distances in between the planes and for similar magnitude of atoms and wavelength of X-rays, constructive and destructive interference phenomena takes place. The X-rays are emitted at particular angles called characteristic angles on the basis of spaces in between the atoms arranged in the crystalline structures called planes.

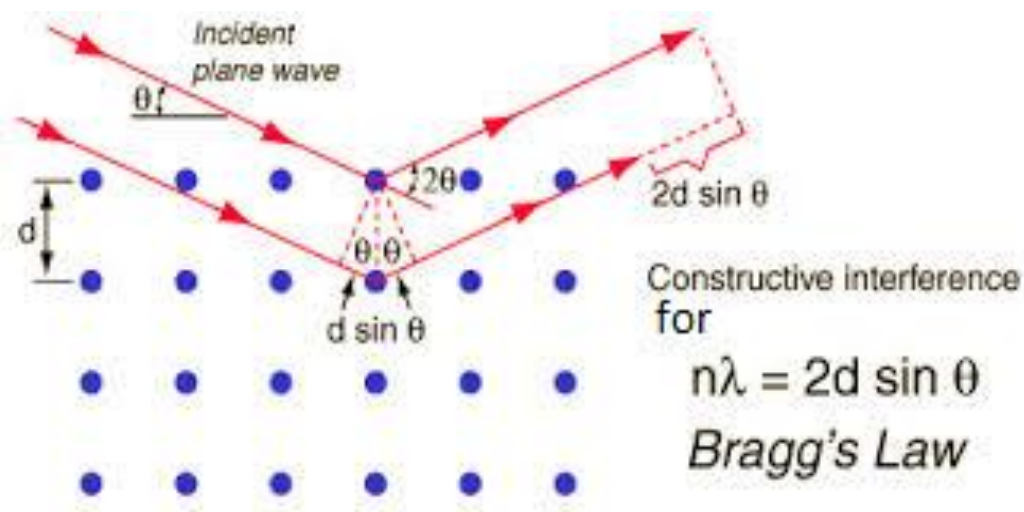


Figure 2.1. Bragg's Law [2]

2.3. SILVER COATING OF THE SENSOR

Silver is a good conductor of electricity. Silver coating has to be applied to all the palletes to make them conducting from both sides of their circular surface. silver coatings were applied on both sides to approximately half the diameter of the pallets. The coatings were circular and at the centre of the sample.

After coating one side of the pallet, it was dried for 120 minutes at 110°C . Then after one side is dried, the other side was coated in the similar manner. Finally the pallets were fired at 650°C for two hours to make the coating stick to the surface ready for electroding.

2.4. COPPER WIRE ELECTRODING

Thin copper wires of approximately 10 cm length were cut from the roll. The ends of each wires were scrapped of its plastic coating to make it conducting from the ends. One end of the scatched wire was soldered on the silver paste to make an electrode and similar process was done for the other side of the pallet, too.

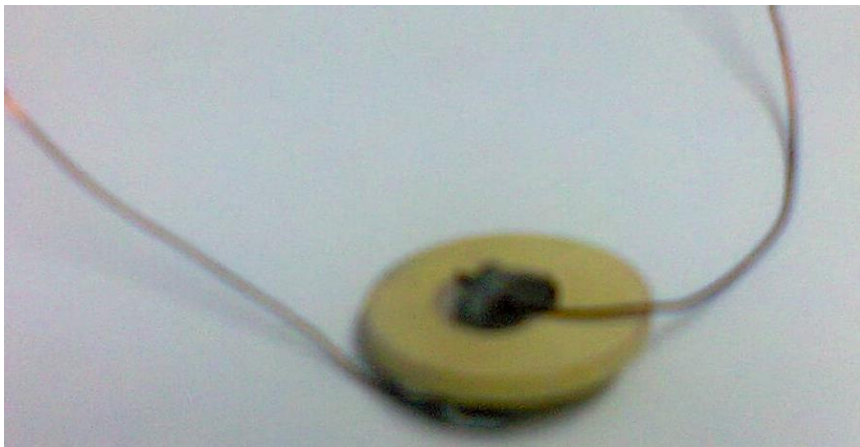


Fig 2.2. Pallates electroded by copper wire

2.5. CREATION OF CONTROLLED HUMID ENVIRONMENT

The controlled humid environment is generated by making supersaturated solution of particular salts at room temperature in a closed vessel. The aquaous solutions of LiCl, MgCl₂, NaBr, NaCl, KCl and K₂SO₄ in a closed glass vessel at room temperature (20 °C), are reported to generate approximately 11%, 33%, 59%, 75%, 85% and 98% relative humidity, respectively.

Table 2.1. supersaturated salt solution vs RH

Supersaturated salt solution	RH (%)
LiCl	11
MgCl ₂	33
NaBr	59
NaCl	75
KCl	85
K ₂ So4	98



Figure 2.4. controlled humid environment

Supersaturated solutions of salts were prepared by adding salt in distilled water till some of it is left undissolved at the bottom. The amount of salt needed for making the supersaturated solution were determined from the following standard table:

Table 2.2. saturated salts vs amount required per 100 ml

Salts to be saturated	Amount required per 100 ml (in grams)
LiCl	127.5
MgCl ₂	57.5
NaBr	121
NaCl	39.8
Kcl	40
K ₂ So4	14.76

After the supersaturated solution is made, it was kept in a clean dessicator at its bottom. The electroded pallets were put on the upper divider plate and nozzle was closed. The set was left at the room temperature for 24 hours and then measurements were taken.

2.6. HUMIDITY SENSING TEST

For measuring the characteristics of humidity responses, an impedance analyzing device, fig 2.5, (model hioki 3532-50 LCR Hi TESTER) using specific software

was used. The operating voltage was maintained at AC 1 V and the operating frequency was changed according to the measurements. Wires from both sides of the pallet were attached to the impedance analyzer and testing window was opened. From the analysis data as impedance(Z), angle(θ), capacitance (C_p) and loss factor(d) were obtained and graphs were plotted between Z' and Z'' where,
 $Z' = Z \cos(\theta)$
 $Z'' = Z \sin(\theta)$.



Figure 2.5. Impedance analyzing device

3. RESULTS AND DISCUSSIONS

3.1. APPARENT POROSITY AND BULK DENSITY

The apparent porosity and bulk density of all the three samples were measured according to the following table:

Table 3.1. Apparent porosity and bulk density

Sample (pallets)	Soaked weight(W)	Suspended weight(S)	Dry weight (D)	Bulk density(g/cc) (D/W-S)	Apparent porosity(%) (W-D/W-S)
$\text{Bi}_{0.5}\text{Li}_{0.5}\text{TiO}_3$	0.4677	0.3790	0.4583	5.26	10.59
$\text{Bi}_{0.5}\text{Na}_{0.5}\text{TiO}_3$	0.9099	0.7214	0.8663	4.59	23.12
$\text{Bi}_{0.5}\text{Na}_{0.25}\text{Li}_{0.25}\text{TiO}_3$	0.8965	0.6901	0.8299	4.02	32.2

The apparent porosity of $\text{Bi}_{0.5}\text{Na}_{0.25}\text{Li}_{0.25}\text{TiO}_3$ is found to be 32.2% which is higher than the single alkaline earth metal co-substituted sites. This result shows that samples are highly porous. High porosity value of sample are very helpful in humidity sensing because it consists more active sites for moisture absorption.

3.2. XRD ANALYSIS

For all the pallets sintered at 800°C, 850°C and 900°C, XRD analysis is done. The primary phase present in the analysis are $\text{Bi}_{0.5}\text{Na}_{0.5}\text{TiO}_3$, $\text{Bi}_{0.5}\text{Na}_{0.25}\text{Li}_{0.25}\text{TiO}_3$ and $\text{Bi}_{0.5}\text{Li}_{0.5}\text{TiO}_3$ respectively. The XRD patterns shows that initial precursor oxides have been completely transformed to the crystalline phases as shown below in fig 3.1, 3.2, 3.3 .

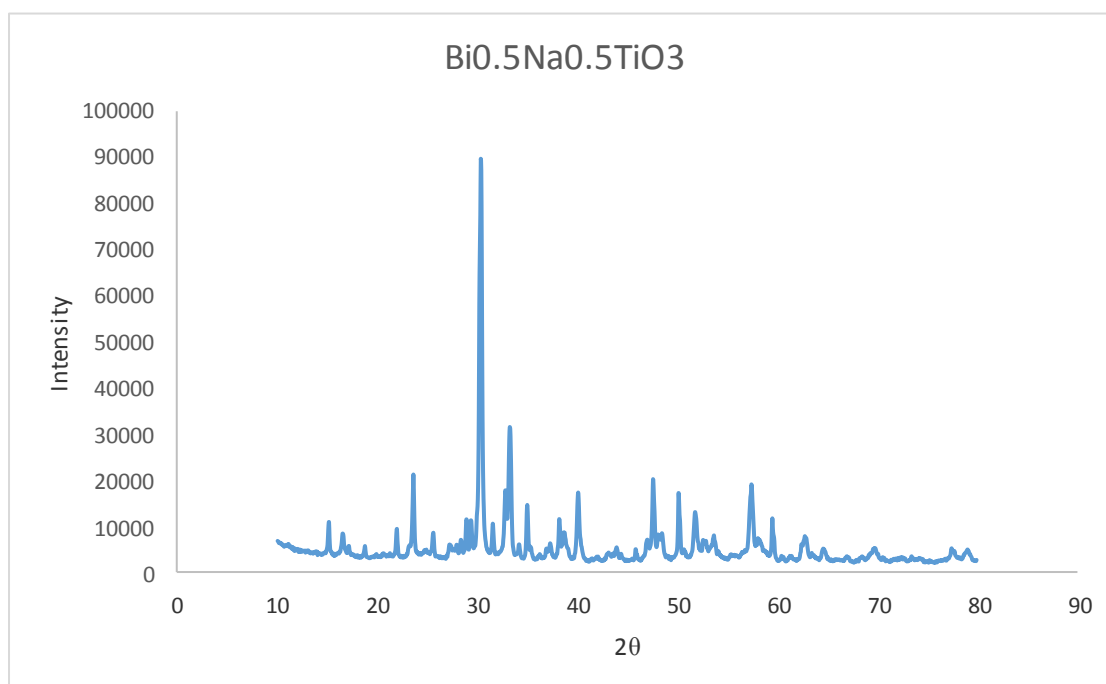


Figure 3.1. XRD for $\text{Bi}_{0.5}\text{Na}_{0.5}\text{TiO}_3$

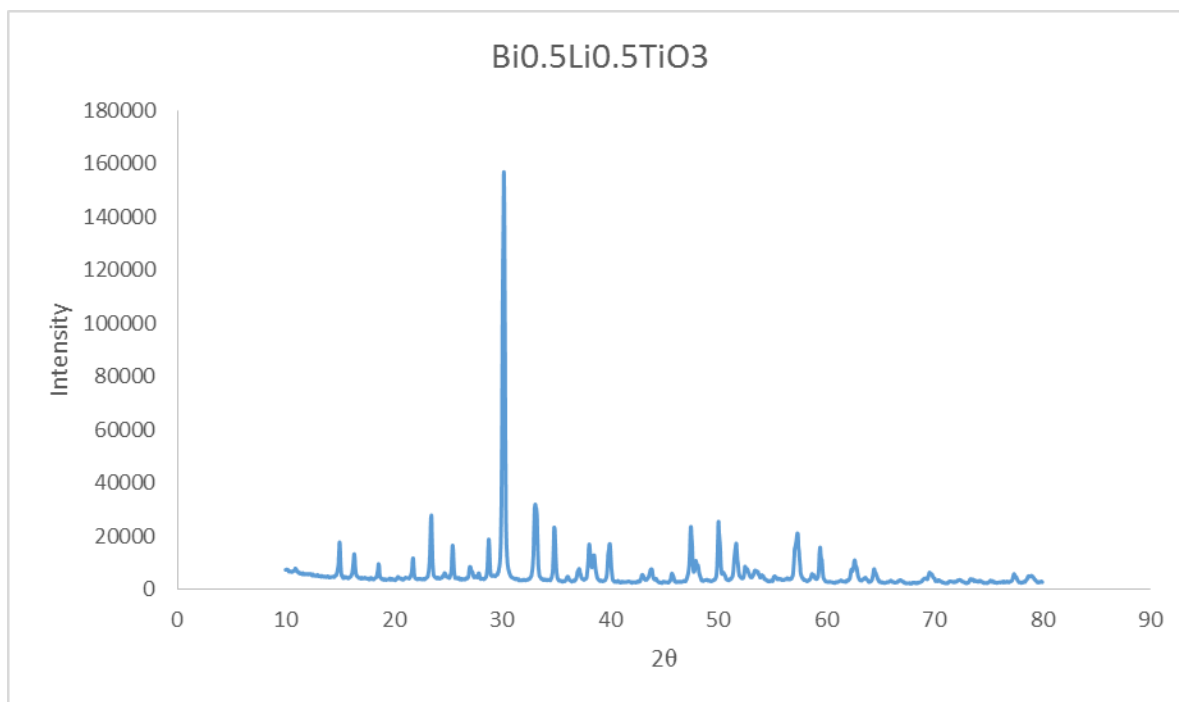


Figure 3.2. XRD for Bi_{0.5}Li_{0.5}TiO₃

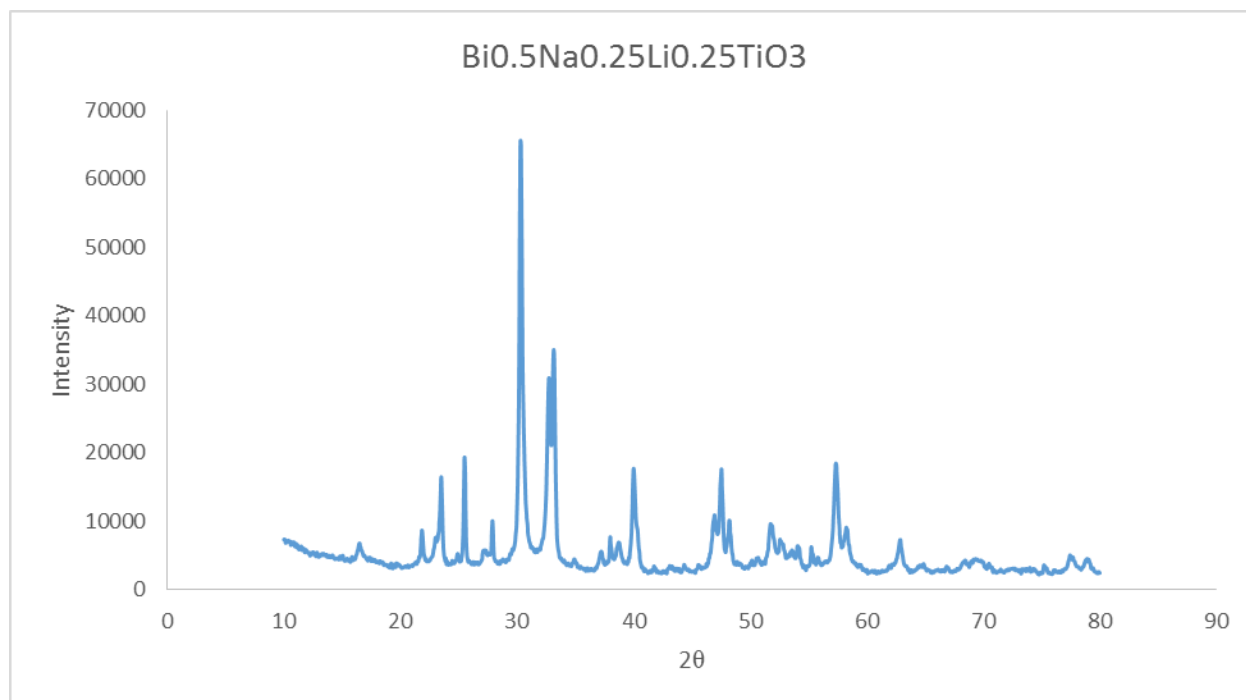


Figure 3.3. XRD for Bi_{0.5}Na_{0.25}Li_{0.25}TiO₃

3.3. SEM ANALYSIS

3.3.1. SEM OF SAMPLE SINTERED AT 800⁰ C ($\text{Bi}_{0.5}\text{Na}_{0.25}\text{Li}_{0.25}\text{TiO}_3$)

Following figure shows that it has highly porous morphology, with pore channel diameter 2-4 micrometers. This implies that the ceramics is highly porous. The micrographs are shown below:

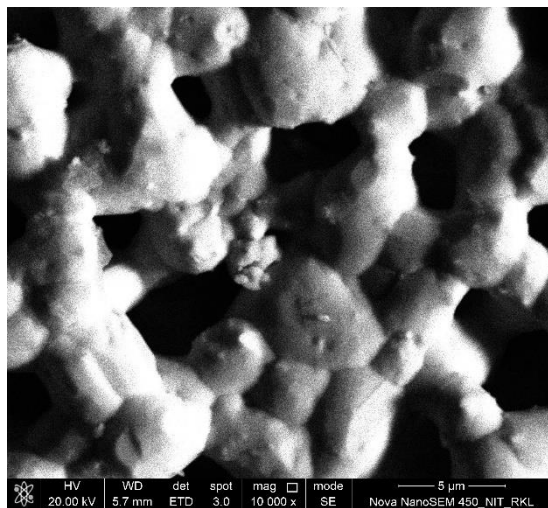
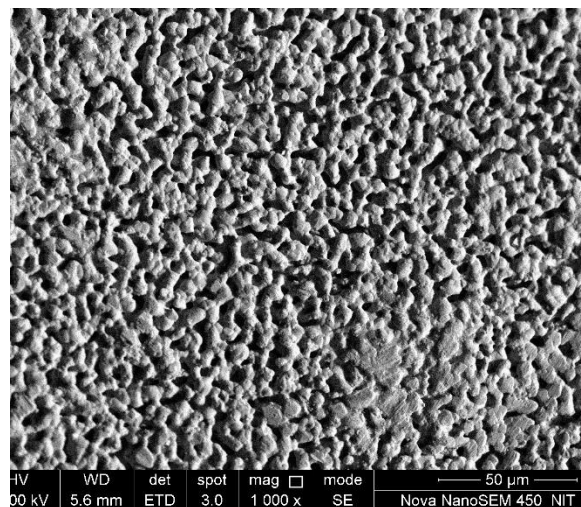


Fig 3.4. 800⁰C SEM micrograph

3.3.2 SEM OF SAMPLE SINTERED AT 850⁰ C ($\text{Bi}_{0.5}\text{Na}_{0.5}\text{TiO}_3$)

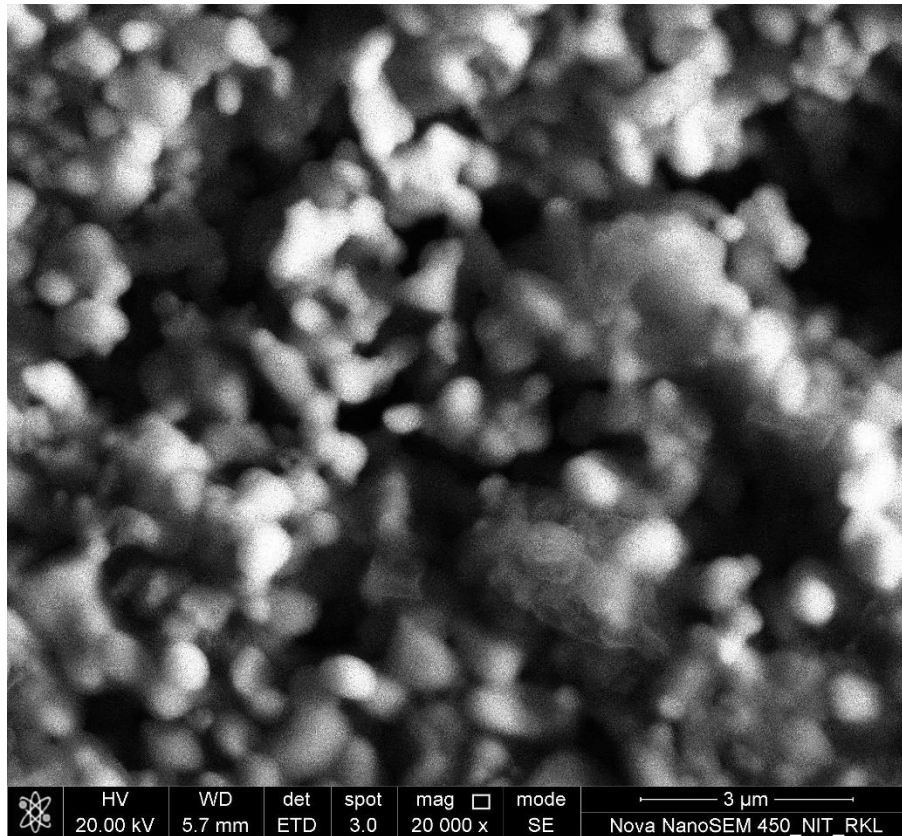


Fig 3.5. 850⁰c SEM micrograph

3.3.3 SEM OF SAMPLE SINTERED AT 900⁰ C ($\text{Bi}_{0.5}\text{Li}_{0.5}\text{TiO}_3$)

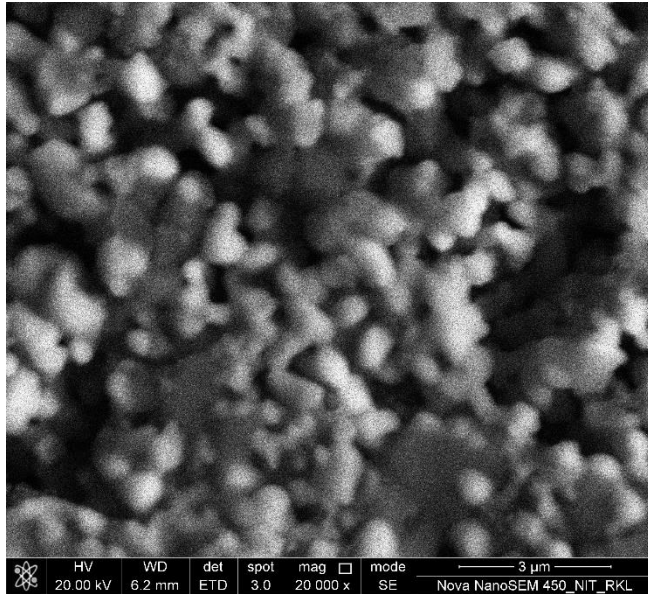


Fig 3.6. 900⁰C SEM micrograph

3.4.HUMIDITY SENSING MECHANISM AND CHARACTERISTIC GRAPHS

The electrical properties of the capacitive ceramic humidity sensors changes with water absorption on its surface. Water molecules are retained on the active sites of the oxide surface chemically forming hydroxyl ion by dissociation mechanism. While, if this happens on the surface of a metal [10], the local density and electric field is changed and the proton reacts with oxygen to form hydroxyl ions. Because of the presence of high electrostatic fields in layers absorbed chemically from

single layer, the water molecules have a tendency to dissociate easily [11]. A surge in the vapor pressure generates dipole under the field applied and results in the increase of dielectric constant [12].

By Kulwicki's theory [13], the conduction process in ceramic and porous materials primarily takes place as surface mechanism, and the large increase in conductivity of $\text{Bi}_{0.5}\text{Na}_{0.25}\text{Li}_{0.25}\text{TiO}_3$ with increase in RH may be due the adsorption of water molecules on the powder surface. The two stages of adsorption are: a) chemisorption and b) physisorption. The polar molecules of water form hydrogen bonds with Oxygen atoms on the surface of the powder and begin to chemisorb. Hydroxyl ion and protons are formed at low humidity when the initial layer of vapor molecules are absorbed [13]. Here the hydroxyl ions are absorbed on the metal surfaces of Na^+ or Li^+ and the protons are absorbed by oxygen ions to form hydroxyl ions again [14]. By the proton conductivity model of Anderson and parks [12, 14], at the absence of water molecules, only protons are able to be formed, and the conduction is taking place at the room temperature because of the proton movement from one site to another passing over the energy barriers of the surface. This explains the very high impedance of the sensor [15].

After the completion of chemisorption, physisorption starts on its own as the layers of water vapor will get physically absorbed with increasing RH. Water molecules act as bulk liquid water after second layer formation due to physisorption. These layers vanish as the humidity is decreased.

$2\text{H}_2\text{O} \leftrightarrow \text{H}_3\text{O}^+ + \text{OH}^-$ is the reaction for dissociation of physisorped water [32]. In the presence of extra adsorbed water, hydration of H_3O^+ takes place. If we follow

the ion transfer mechanism of Grotthuss [33], both the starting and ending states are the same: $\text{H}_2\text{O} + \text{H}_3\text{O}^+ \rightarrow \text{H}_3\text{O}^+ + \text{H}_2\text{O}$.

Transfer of H_3O^+ is easier because of the equivalence of energy.

But, concurring with the ion transport model given by Casalbore-Miceli et al. [15], the powder may get dissolved in the water adsorbed, and the conduction carriers are the dissociated ions like Na^+ . Hence the impedance of the humidity sensor based on $\text{Bi}_{0.5}\text{Na}_{0.25}\text{Li}_{0.25}\text{TiO}_3$ continuously goes down when compared to the initial impedance results with increasing RH.

Sodium, an alkali metal gets easily dissolved to water. The solubility is very high and higher solubility of dopants improves the sensing properties and different theories have been put forward in its support [15, 16].

In some cases, the addition of alkali ions was reported to affect the microstructure of the material, causing changes such as the specific surface area, grain size, average pore size, etc. [16] and thereby resulting in improved humidity sensitivity. Yeh and Tseng thought that the addition of alkali ions could create more surface defects and oxygen vacancies, resulting in an increase of the number of adsorption sites for water molecules [17]. In our case, compared with the previously reported powder [18], the obvious microstructure changes were observed for the powder. The microstructure of sample powder is of homogeneous spherical microstructure with some fragments attached on it, which may be helpful for the increase of the specific surface. Moreover, we expect that the improved humidity sensing performance is also related to the direct contribution of Na^+ to the conduction. At low RH, Na^+ can provide more charge carriers for hopping transport [2, 7]. At high RH, Na^+ may dissolve in the adsorbed water, and play the roles of conduction carriers.

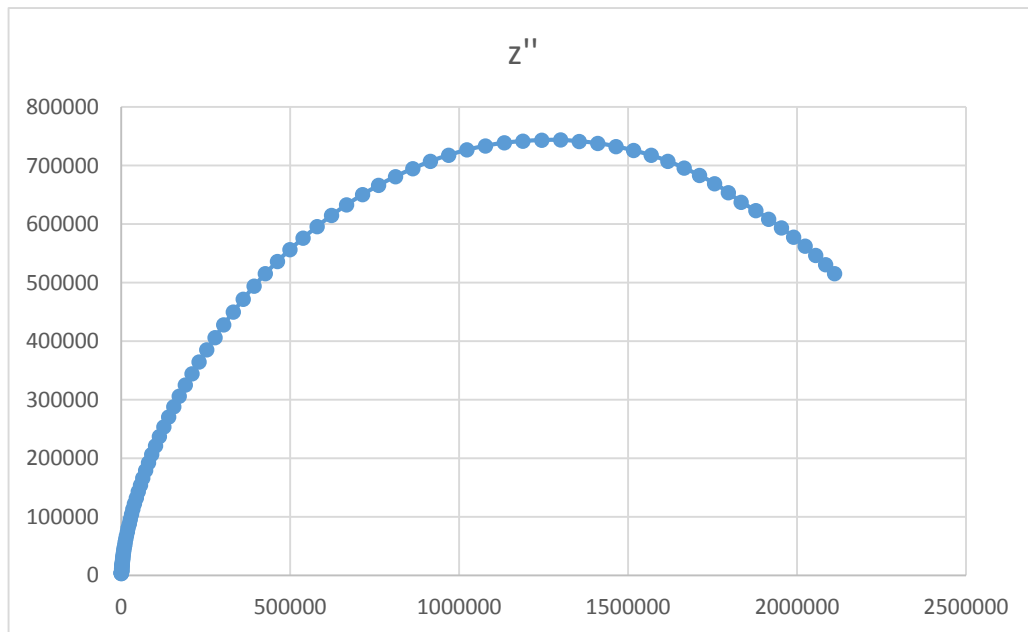


Figure 3.7. impedance spectra with 33% RH

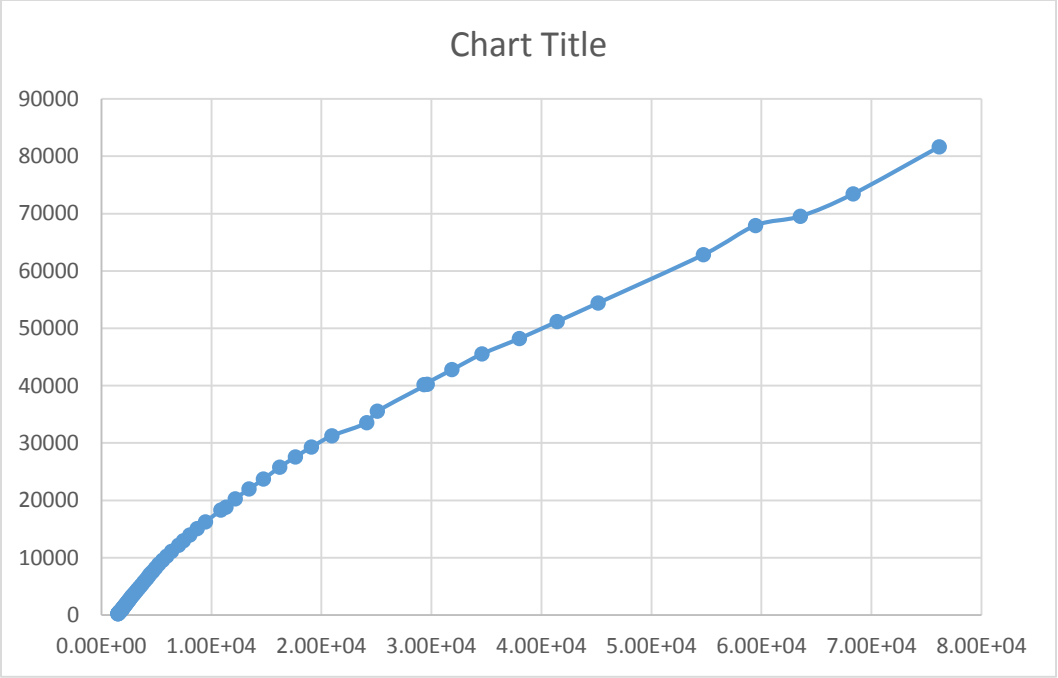


Figure 3.8. impedance spectra with 75% RH

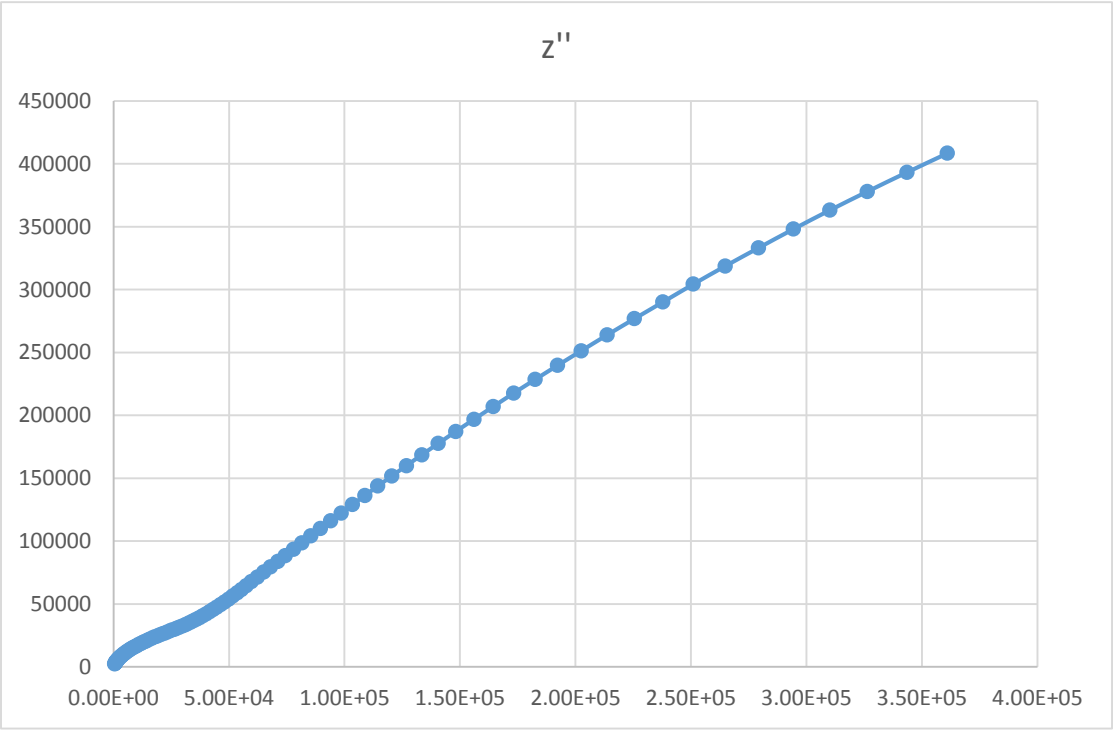


Figure 3.9. impedance spectra with 85% RH

For demonstrating above analysis, the impedance plots of $\text{Bi}_{0.5}\text{Na}_{0.25}\text{Li}_{0.25}\text{TiO}_3$ were made in the frequency range varying from 100 Hz to 100 kHz with RH variations of 33%, 75% and 85% . ReZ and ImZ are the real part and imaginary part of the complex impedance. In order to show the complex impedance plots clearly, the scales in Figures are different. When the RH increased to 33%, the curvature radius of the arc reduces, and the most part of semicircle is observed in Fig. 3.4, 3.5, 3.6 . The semicircles disappear entirely, and only the lines are observed at 75%, and 85% RH. The appearance of the semicircle fig. 3.4 indicates an equivalent circuit consisting of parallel combination of resistance and capacitance components and, and testifies the existence of ionic conduction (H^+ hopping).. Due to the active electrolytic conduction, the semicircle became ignorable under rather high humidity conditions [13], and the Warburg impedances caused by the diffusion of the electroactive species at the electrodes are represented as the lines. From the complex impedance plots analysis, we ascertain that the experimental results are in accordance with the theorized model above.

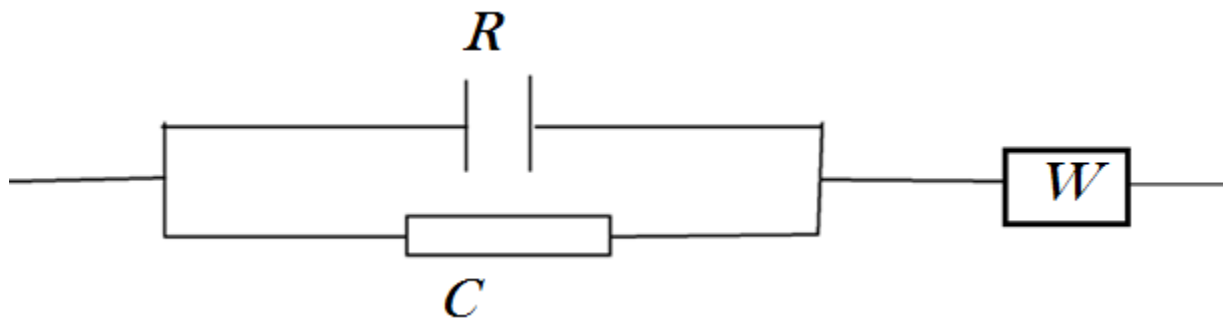


Figure 3.10. Equivalent circuit design

The impedance dependency of the fabricated samples on the measured relative humidity for the sensor by using $\text{Bi}_{0.5}\text{Na}_{0.25}\text{Li}_{0.25}\text{TiO}_3$ ceramic humidity sensor having mesoporous structure was measured at various frequencies, as shown in below in figure 3.8.

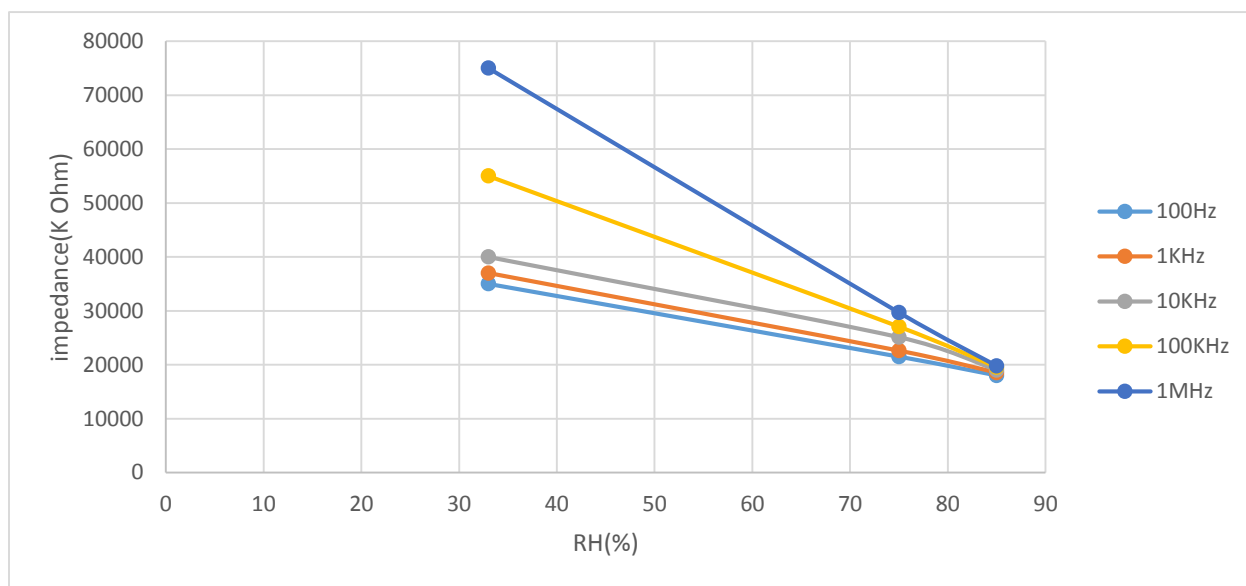


Figure 3.11. impedance vs relative humidity

4. Conclusion

$\text{Bi}_{0.5}\text{Na}_{0.25}\text{Li}_{0.25}\text{TiO}_3$ based humidity sensor was successfully synthesized via the solid state sintering method. The characterization and humidity sensing properties of the $\text{Bi}_{0.5}\text{Na}_{0.25}\text{Li}_{0.25}\text{TiO}_3$ based humidity sensor are provided. The sensor exhibits good sensing properties. Disc shaped humidity sensors was fabricated and tested of its sensing characteristics. . The impedance changes by more than four orders of magnitude in the range of 33-85 % RH, which will be suitable for fast response time, high response and longtime stability.

REFERENCES:-

- [1] <http://www.engineersgarage.com/articles/humidity-sensor>
- [2] <http://en.wikipedia.org/wiki/Humidity>
- [3] Ceramic sensor humidity detector the state art and future development, Sensor and Actuator E. Traversia, B 23 (1995) 135 156
- [4] Electrical and electronic sensing property of a flexible humidity sensors made of polyamido amine dendrimer–Au nanoparticles, P.G. Sui, C.C. Sheu Sensor and Actuator B 165 (2012) 151–156.
- [5] Optimizational analysis of calorimetric photonic of crystals humidity sensors fabricated by glancing angled deposition, Advanced Engineering Materials Mr. Hawkeye, P.J. Brett, 21 (2011) 3652 3658.
- [6] Fiber optical sensor advanced technologies for humidity measurement and moisture measurements, Sensor and Actuator T.J.L. Yeo, T. Suin, K.I.V. Gaitan, A 144 (2008) 280 295.
- [7] Water Vapour Measurements & Method and Instrumentation, Marcel Dekker, New Yorks, P.R. Weederhold, 1997.
- [8] Relative and specific humidity sensor based on an environmental and sensitive fluorophore materials in hydrogen gel thick films, Analytical Chemistry J.C. Telis, C.A. Stollson, M.N. Myeers, K.I.A. Kneas, 83 (2011) 928 932.

- [9] The relation between the amount of chemic-absorbed and physic-absorbed water on metal oxides, T. Morimooto, M. Naagao, F. Tookuda, Journal of Physical and general Chemistries 73 (1969) 243 248.
- [10] B.N.B. Kulwihcki, ceramic Humidity sensots, Journalis of Americans Ceramis cociety 74 (1991) 697 706.
- [11] Highliy sensitivie ceramic humidity sensor depending on amorphous Al₂O₃ nanotubes, Journals of Material science Chemistry , B. Cheing, B. Tan, C. Xiaee, Y.r. Xiao, S. l.Lei, 21 (2011) 1907 1912.
- [12] Theoretical study on the impedance versus humidities characterisation of humidiity sensor, Sensor and Actuator Y. Simizu, H. t.Arai, T. Seyama, 7 (1985) 11–22.
- [13] Synthesis process and characterization of semiporous indiuim tin dioxide porssessing an electronic conductive frameworks, i.T. Eonns, J.Q. Li, L.c.F. Najar, 124 (2002) 8516–8517.
- [14] Rapid Prototyping Journal, Volume 17, Issue 3 (2011-05-01)
- [15] Traversa, E.. "Ceramic sensors for humidity detection: the state-of-the-art and future developments", Sensors & Actuators: B. Chemical, 199502
- [16] Y. Zhang, X.J. Zheng, T. Zhang, L.J. Gong, S.H. Dai, Y.Q. Chen
Humidity sensing properties of the sensor based on Bi_{0.5}K_{0.5}TiO₃ powder
Sens. Actuators B Chem., 147 (2010), pp. 180–184
- [17] T.Y. Kim, D.H. Lee, Y.C. Shim, J.U. Bu, S.T. Kim Effects of alkaline oxide additives on the microstructure and humidity sensitivity of MgCr₂O₄–TiO₂
- [18] Y. Sakai, M. Matsuguchi, N. Yonesato Humidity sensor based on alkali salts of poly(2-acrylamido-2-methylpropane sulfonic acid)

